Article

Exploring the antibacterial and antibiofilm efficacy of silver nanoparticles biosynthesized using *Punica granatum* leaves

Monisha Singhal [1], Sreemoyee Chatterjee [1], Ajeet Kumar [2], Asad Syed [3], Ali H. Bahkali [3] Nidhi Gupta [1,*], and Surendra Nimesh [4,*]

[1] Department of Biotechnology, IIS (Deemed to be University), Gurukul Marg, SFS, Mansarovar, Jaipur 302020 Rajasthan, India

[2] Department of Chemistry and Biomolecular Science, Clarkson University, Potsdam, NY 13699-5814

[3] Department of Botany and Microbiology, College of Science, King Saud University, P.O. 2455, Riyadh 11451, Saudi Arabia Department of Biotechnology, School of Life Sciences, Central University of Rajasthan, Ajmer 305817, India

[4] Department of Biotechnology, School of Life Sciences, Central University of Rajasthan, Ajmer 305817, India

* Correspondence: Nidhi Gupta - nidhinimesh@gmail.com or nidhi.gupta@iisuniv.ac.in , Surendra Nimesh - surendranimesh@gmail.com or surendranimesh@curaj.ac.in; Tel.: +91-9468949252; Fax: +91-1463-238722

Abstract: The current research work illustrates an economic and rapid approach towards biogenic synthesis of silver nanoparticles using aqueous *Punica granatum* leaves extract (PGL-AgNPs). The optimization of major parameters involved in the biosynthesis process was done using Box-Behnken Design (BBD). The effects of different independent variables (parameters) namely concentration of $AgNO_3$, temperature and ratio of extract to $AgNO_3$on response viz. particle size and polydispersity index were analyzed. As a result of experiment designing, 17 reactions were generated which were further validated experimentally. The statistical and mathematical approaches were employed on these reactions in order to interpret the relationship between the factors and responses. The biosynthesized nanoparticles were initially characterized by UV-vis spectrophotometry followed by physicochemical analysis for determination of particle size, polydispersity index and zeta potential via dynamic light scattering (DLS), SEM and EDX studies. Moreover, the determination of functional group present in the leaves extract and PGL-AgNPs was done by FTIR. Antibacterial and antibiofilm efficacies of PGL-AgNPs against Gram-positive and Gram-negative bacteria were further determined. The physicochemical studies suggested that PGL-AgNPs were round in shape and of ~ 37.5 nm in size with uniform distribution. Our studies suggested that PGL-AgNPs exhibit potent antibacterial, and antibiofilm properties.

Keywords: *Punica granatum* leaves extract, silver nanoparticles, Box-Behnken design, antibacterial, antibiofilm

1. Introduction

Nanotechnology deals with manipulations of materials at molecular and sub-molecular levels. It is primarily concerned with the development of natural and artificial nanostructures. The nanoparticles explicitly lie in the size range of 1nm to 100nm in any one dimension and possess features that vary from their bulk counterpart. The properties of nanoparticles tend to change due to reduction in size and structure of the materials to the atomic level. This has made them compatible for various applications such as diagnostic tools, vehicles for drug loading, biosensors,

sunscreens formulation, antimicrobial therapeutics in the form of bandages and disinfectants, and as catalyst. These nanoparticles therefore, offer greater efficiency in the manufacturing process as the use of toxic materials can be reduced [1]. Metallic nanoparticles, specifically silver nanoparticles (AgNPs) have been utilized in various applications due to its unique broad spectrum antibacterial and antifungal activity. These inorganic nanoparticles exhibit low toxicity against mammalian cells as compared to its bulkier salt form [2]. AgNPs are well known to show their effectiveness against multidrug resistance bacteria.

Various chemical and physical methods are available for the synthesis of these AgNPs that are capable of producing well defined, small sized nanoparticles. But all these methods are associated with certain limitation as these are very costly, energy consuming and utilize hazardous chemicals. Aside from these limitations, low stability and aggregation of the formulated nanoparticles is another challenge [3]. To combat these issues, researcher are now moving towards the biological synthesis of these AgNPs including microbial (bacteria, fungi based) synthesis and green (plant-based) synthesis [4].

Plants extract, have the ability to reduce and act as capping agent during nanoparticles synthesis and are considered advantageous over microbial synthesis owing to its less cumbersome process [5].Thus, the elaborated process of culture and maintenance of microorganisms can be avoided and plant extract mediated synthesis can easily be amplified for larger scale [5]. Different types and parts of plant such as, *Prosopis juliflora* bark, *Prosopis juliflora* leaf, *Cicer arietinum* leaves, *Trigonella foenum-graecum* seed, *Terminalia chebula* fruit, *Saraca indica* flower, *Punica granatum* peel, *Acacia nilotica* leaf etc. have been used for biosynthesis of AgNPs [6]. Not only the plant parts but the waste from the plants have also been explored for biosynthesis of AgNPs such as lignin extracted from wheat straw and grape pomace from the wine industry [7]. Various biomolecules (such as polysaccharides, polyphenols, aldehydes, ketones, proteins/enzymes, amino acids and caffeine) present in the extracts play a vital role in reduction of metal ion and stabilize the nanoparticles [8]. *Punica granatum* (common name, Pomegranate), is a small fruit-bearing deciduous shrub that belongs to *Punicaceae* family. *P. granatum* leaves contain tannins, flavones, apgenin, luteolin, glycosides which enables it to have a wide range of potential health benefits. It has been shown to aid in digestion and treat certain infections and illness. In a recent study, the leaves of *P. granatum* were used for the biosynthesis of AgNPs and explored for their antidiabetic, anticancer and antibacterial potential [9]. In another study, the peel waste of *P. granatum* was employed for biosynthesis of AgNPs and the antibacterial potential explored against both Gram negative and Gram positive bacteria along with evaluation of its cytotoxicity against a colon cancer cell line, RKO [10]. A further study reported use of Punicalagin, found in *P. granatum* husk for synthesis of AgNPs and exploration of its antioxidant, antibacterial, and anti-cancer potential against HepG2 cancer cells [11].

Though few studies have reported use of *P. granatum* leaves, peel or husk for biosynthesis of AgNPs, a systematic study that examines the influence of various parameters that dictates the size of AgNPs such as concentration of $AgNO_3$, temperature, ratio of extract to $AgNO_3$ is lacking. The present study was designed to critically investigate the influence of several parameters determining the size of nanoparticles (PGL-AgNPs) such as concentration of $AgNO_3$, temperature, ratio of extract to $AgNO_3$. The novelty of the present work relies on the application of Box-Behnken design (BBD) for the optimization of these parameters in the biosynthesis process. The biosynthesis of AgNPs from $AgNO_3$ was observed using UV-vis spectroscopy. Physicochemical characterization of PGL-AgNPs in terms of size and size distribution along with zeta potential was done on DLS, SEM followed by energy dispersive X-ray spectroscopy (EDX), FTIR and XRD. FTIR was further explored to identify the modulation in the bacterial biomolecules that could occur due to exposure to biosynthesized AgNPs. The antibacterial activity of PGL-AgNPs was studied against *Bacillus subtilis*, *Staphylococcus aureus, Pseudomonas aeruginosa, Escherichia coli*, and *Proteus vulgaris.* Further, the antibacterial mechanism of PGL-AgNPs was deciphered using SEM. Finally, the antibiofilm efficacy was also explored in two biofilm forming bacteria i.e. *P. aeruginosa* and *S. aureus*.

2. Results and discussion

2.1. Biosynthesis of PGL-AgNPs

The leaves of *P. granatum* are known to contain several tannins, flavones, apgenin, luteolin, glycosides etc. that could apparently assist in the formulation of AgNPs. The AgNPs genesis was marked by the steady transition in color of the reaction mixture from greenish yellow to dark brown with peculiar surface plasmon resonance (SPR) peak around 420 nm, further confirming its formation **(Fig. 1)**. Arya *et al.* have suggested change in color from light yellow to dark brown due to formation of AgNPs using *Prosopis juliflora* leaf extract [6f]. In another study, Ahmed *et al.* have also shown color transformation in case of colorless $AgNO_3$ solution to dark brown as a result of AgNPs formation where *Terminalia arjuna* bark extract was employed [12]. In one of the study, Arya *et al.* reported optimum synthesis of AgNPs using *Prosopis juliflora* leaf extract at 25°C where 0.5 ml of extract was used to reduce 9.5 ml of $AgNO_3$ (1mM) when reaction sustained for 40 min [6f]. In another study, Veisi *et al.* used aqueous leaf extract of *Thymbra spicata* and reported that for optimum synthesis 30 min were required for entire reduction of $AgNO_3$ [13]. Biosynthesis of AgNPs using *Garcinia mangostana* leaf extract was also tested for its antimicrobial activities [14]. Chand *et al.* reported a study where they biosynthesized AgNPs using onion (O), tomato (T), acacia catechu (C) alone and mixture of all three (COT) extracts [15].

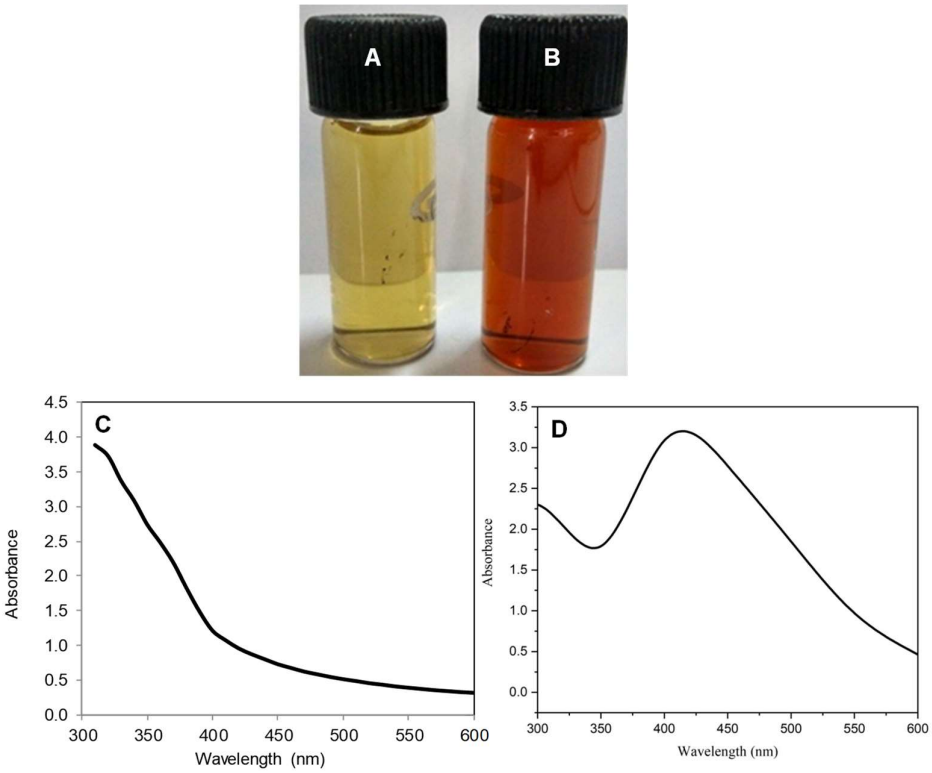

Figure 1. Color change showing biosynthesis of PGL-AgNPs, A-PGL leaves extract, B-PGL-AgNPs resuspended in double distilled water, C- UV-vis spectrum of PGL leaves extract, and D-UV-vis spectrum of synthesized PGL-AgNPs with peak around 420 nm.

2.2. Box-Behnken design for optimization of parameters for biosynthesis of PGL-AgNPs

Optimization of parameters for AgNPs biosynthesis is essential in order to improve the stability of the prepared nanoparticles along with minimal variability in terms if size. The optimization also facilitates enhancement in the nanoparticles yields that would be one essential prerequisite in case of bulk synthesis. The systematic optimization of parameters for synthesis of PGL-AgNPs was conducted through BBD by Design Expert version 12.0 (Stat-Ease Inc.,

Minneapolis, USA). In this study, 17 trial runs were suggested by BBD where concentration of $AgNO_3$ (mM), reaction temperature (°C) and ratio of extract to $AgNO_3$ (µl) were picked up as independent factors. These 17 reactions were validated experimentally and reactions analyzed for size on DLS. The data procured was further analyzed using quadratic polynomial model and model diagnostic plots were generated to evaluate if the selected model fitted well for the given data. The model diagnostic plots for response particle size were shown in **figure 2A, B, C**. Here, we obtained a linear predicted vs. actual graph indicating that predicted values were very much in close proximity with the predicted ones. The effect of all the selected factors at a particular point in experiment design was predicted by perturbation plot. The graph shows a slight curvature for factor C (i.e. temperature) indicating response's sensitiveness to that particular variable. While other two factors (i.e. A-$AgNO_3$ concentration and B- extract to $AgNO_3$ ratio) was relatively flat indicating no such effects on response when the variables fluctuates. Also, there was no significant mean effect between $AgNO_3$ concentration and extract to $AgNO_3$ ratio as the green and red mean line was parallel to each other as displayed in interaction plot.

Similarly, model diagnostic plots of response polydispersity index (PDI) were generated. **Figure 2D, E, F** illustrates predicted vs. actual plot where experimental values obtained were quite close with the predicted values. The perturbation plot was found to be much deviated as all the factors showed curvatures from the desired point which means change in any factor affect the response to a certain extent. Interaction plot revealed significant mean effect among two selected variables as the mean effect lines intersects with each other.

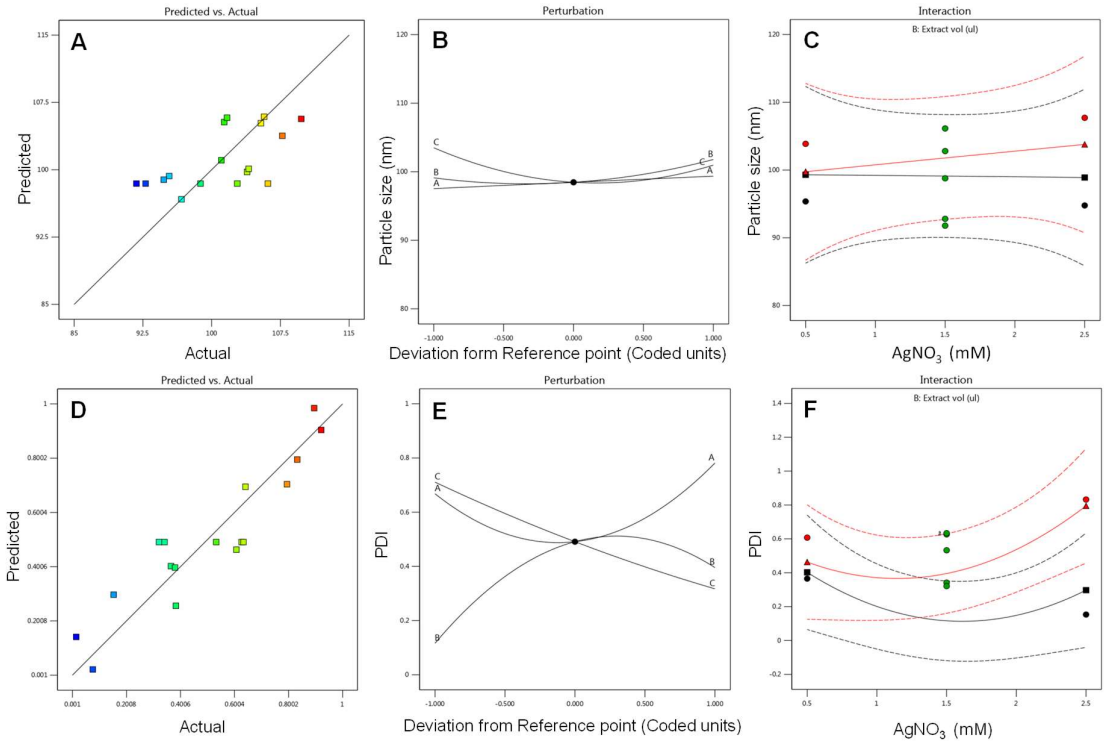

Figure 2: Model diagnostic plots predicted v/s actual, perturbation and interaction plots for response variables- (A) particle size and (B) PDI for *P. granatum* leaves extract mediated silver nanoparticles.

2.3. Factor- response association and response surface analysis

Box and Wilson in 1951 introduced response surface methodology (RSM) as a tool which combines mathematical and statistical approaches to optimize variables or factors for a given model system [16]. Here the existence of all the possible interactions amongst the three independent variables with their impact on responses was evaluated by 2D contour plots and 3D response

surface plots. In **figure 3A, D** the effect of $AgNO_3$ concentration and extract to $AgNO_3$ ratio on response particle size was determined. 3-D response surface plot depicts that there was no such association of both the variables on particle size yet particle size slightly increase at higher levels. 2-D contour plot also predicts the maximum number of particles formation at higher levels. The link between $AgNO_3$ concentration and temperature is shown in **figure 3B, E**. It has been seen that elevating the $AgNO_3$ concentrations at low level of temperature, declining pattern of particle size was observed. Whereas at higher temperature, increase in $AgNO_3$ concentration showed an inclination pattern of particles size. 2-D contour plot also revealed the same relationship. The relationship between extract to $AgNO_3$ and temperature was depicted in **figure 3C, F**. Increasing the volume of extract at lower range of temperature showed a drop in pattern of particle size whereas increasing the extract volume at higher level of temperature, increment in particle size was observed.

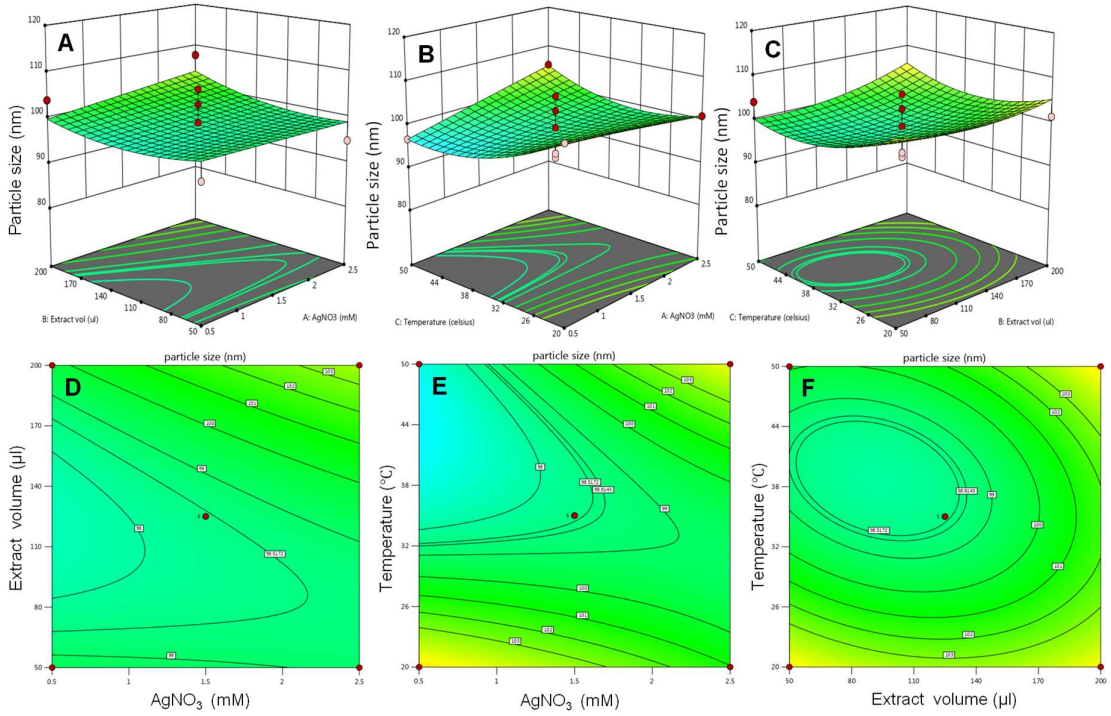

Figure 3. 3D surface plot and 2D contour plots for response- particle size

Similarly, the influence of all three variables on response polydispersity index was evaluated. In **figure 4 A, D**, 3-D surface plot showed a complex interaction between $AgNO_3$ concentration and extract to $AgNO_3$ ratio where increased concentration of $AgNO_3$ at lower levels of extract volume, a declining pattern of PDI was observed. However, rising the concentration of $AgNO_3$ at high level of extract volume, inclining pattern of PDI was observed. **Figure 4B, E** predicts the effect of $AgNO_3$ concentration and temperature on PDI. Increase in concentration of $AgNO_3$ at lower level of temperature exhibit low range of PDI while at higher level of temperature low range of PDI was observed. In **figure 4C, F**; increasing extract volume at low temperature level, PDI tend to increase while increasing extract volume at high temperature level declining pattern of PDI was seen.

2.4. Studies for optimized PGL-AgNPs

The optimization of parameters for PGL-AgNPs biosynthesis was attained by numerical optimization through BBD. Once the experimental validation of 17 reactions was done, the obtained data for responses –Particle size and PDI was subjected to numerical optimization. Herein, the data was adjusted in desired range and an overlay plot was generated to depict the desired conditions for biosynthesis purpose. In **figure 5**, the yellow region predicted the optimized area for

biosynthesis of silver nanoparticles. The plot depicts that desired range of PDI i.e. below 0.3 was obtained at higher concentration of $AgNO_3$ while keeping extract volume at lowest range. The flagged point describes the optimized parameters for the same. As a result, the uniformly distributed nanoparticles can be biosynthesized when the concentration of $AgNO_3$ is 1.5 mM, with extract volume of 55.55 µl was taken and reaction was carried out at 31.4°C continued for 15 min.

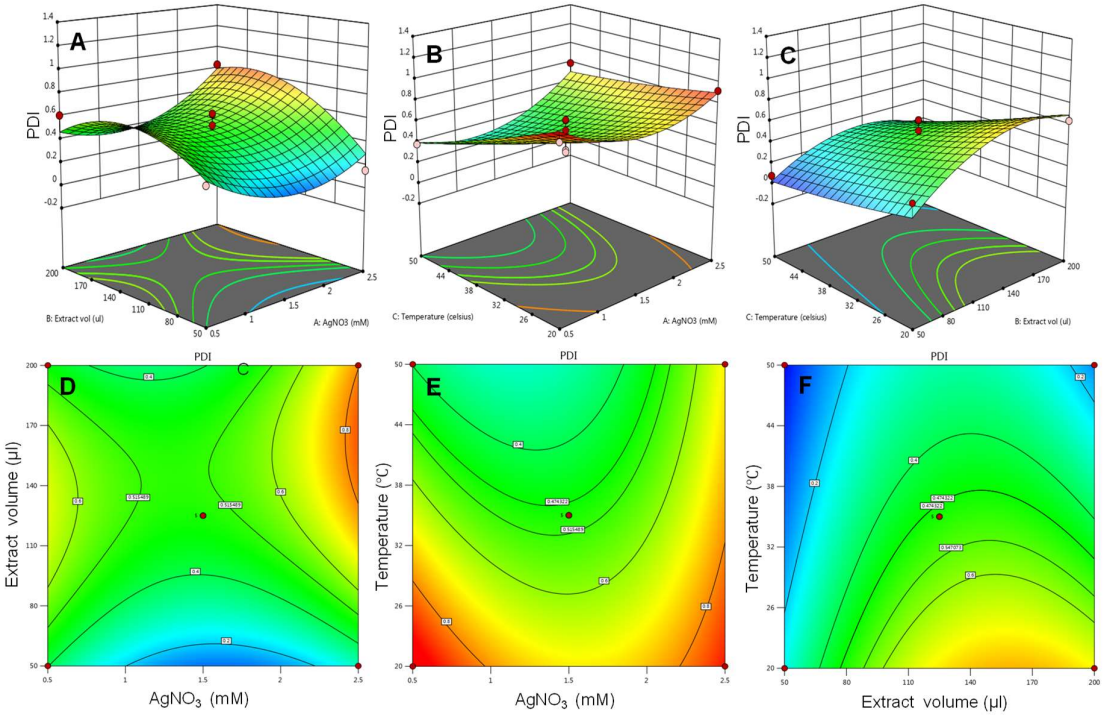

Figure 4. 3D surface plot and 2D contour plots for response- PDI

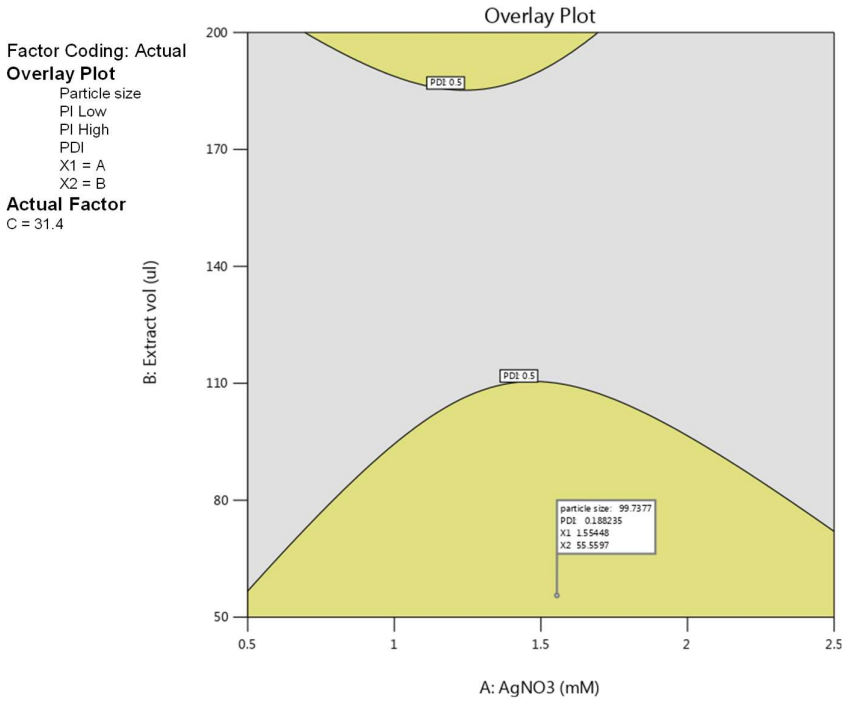

Figure 5. Overlay plot with a flagged point showing optimal conditions for biosynthesis of PGL-AgNPs.

2.5. Physicochemical characterization of PGL-AgNPs

UV-vis spectroscopy is routinely employed for characterization of metallic nanoparticle as they display SPR in the visible light spectrum. SPR is an optical approach widely practiced for determination of molecular interactions in nanoparticles. It is based upon cumulative oscillation of free electrons found on the surface of metal nanoparticles that determines the SPR bands. A narrow size distribution of AgNPs is typically depicted by a sharp peak. This peak may vary with the type, size and shape of nanoparticles. The size of particles and dielectric medium are two main factors, broad peak and prominently small peak depicts vast and mono-dispersed distribution of nanoparticles, respectively [17]. In event of spherical nanoparticles, a single SPR peak is likely to appear while more than two peaks appear in the event of anisotropic nanoparticles [18].

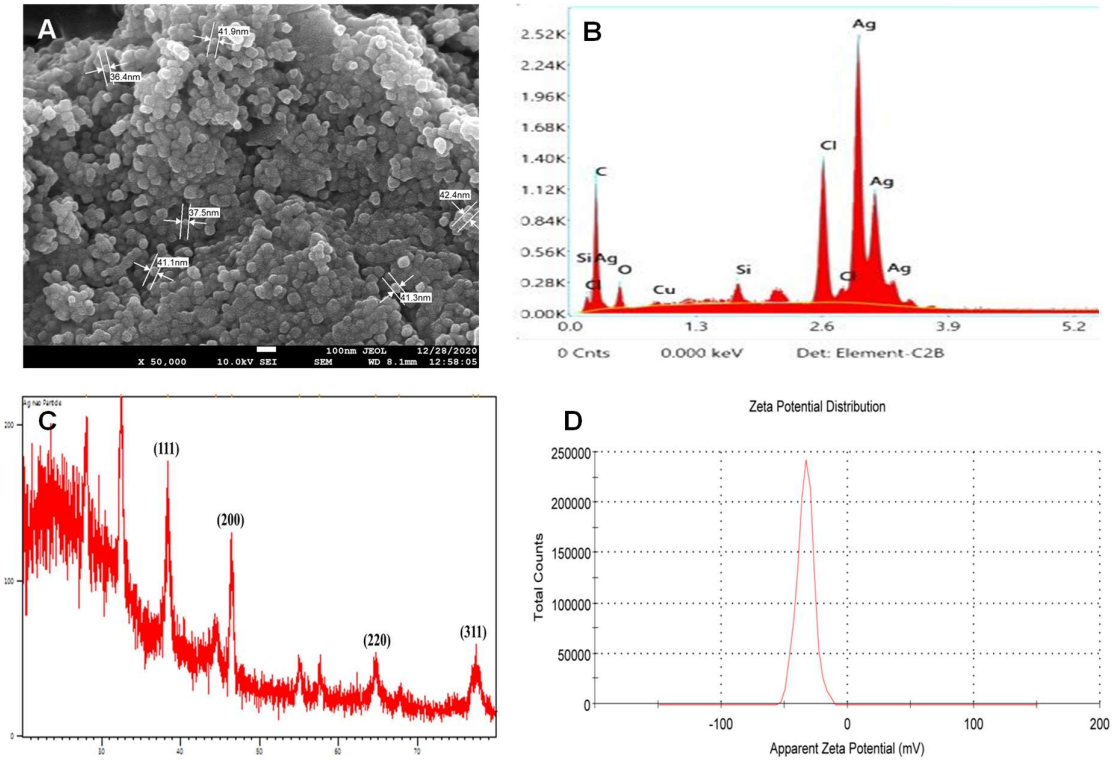

Figure 6. Characterization of PGL-AgNPs synthesized at optimal conditions i.e. 25oC when the concentration of AgNO3 is 1.0 mM, at extract to AgNO3 ratio of 1:10 and reaction continued for 15 min. (A) SEM image of PGL-AgNPs, average size of ~37.5 nm (B) EDX pattern of PGL-AgNPs, (C) XRD spectrum of AgNPs (D) Zeta analysis showing zeta potential is 34 mV

In the present study, reaction mixture showed an absorbance peak at around 420 nm, which is distinctive of AgNPs, due to its SPR absorption band. Size determination studies done on SEM showed that PGL-AgNPs were spherical with smooth surface morphology with an average size of~37.5nm (**Figure 6A**). EDX analysis of biosynthesized nanoparticles revealed the presence of silver atoms (**Figure 6B**). Further, the zeta potential was found to be -34 mV upon analysis of samples on Zetasizer **(Figure 6D)**. XRD study of the PGL-AgNPs disclosed prominent peaks corresponding to (111), (200), (220) and (311) Bragg's reflection based upon the fcc structure of AgNPs **(Figure 6C)**. AgNPs synthesized using *Rheum turkestanicum* shoots extract by Yazdi *et al.* also reported the four Bragg diffraction values 38.2, 44.6, 224 64.6, and 77.5 at 2Θ representing the (111), (200), (220), and (311) set of lattice plane, respectively [19].The synthesis of AgNPs is generally illustrated by expansion of Bragg's peaks. The XRD data received for PGL-AgNPs was compared with the database of Joint Committee on Powder Diffraction Standards (JCPDS) file No. 04-0783. Further, the stability of AgNPs was checked in terms of analysis on UV-vis spectrophotometer after

an interval of 30 days of storage at room temperature. No comparative shift in the spectrum was observed for stored AgNPs in contrast with the freshly prepared AgNPs.

2.6. Fourier-transform infrared spectroscopy

The FTIR spectrum of *P. granatum* leaves extract and PGL-AgNPs was recorded within the range of wavenumber of 4000-400 cm^{-1} region.The AgNPs showed major peaks at 1623 cm^{-1} (N-H bend), 1191 cm^{-1} (C-O stretch), 1025.5 cm^{-1} (C-N stretching) and 756 cm^{-1} (C-Cl stretching) suggesting the relationship of primary amines, aliphatic amines and alkyl halides of the constituting biomolecules present in the extract **(Figure 7)**. N-H stretching comparable to primary and secondary amines was found in both extract and AgNPs which implies that they might be liable for capping and stabilization of PGL-AgNPs. In the PGL extract, the band at 3275 cm^{-1} was attributed to the polyphenols while in the PGL-AgNPs the vibration band moved toward shorter frequency of 3219 cm^{-1} suggesting the implication of functional groups associated with polyphenols as reducing agent during biosynthesis of AgNPs [20]. The band at 2933 cm^{-1} due to O-H stretching vibration, band at 1705cm^{-1} due to C=O stretching vibration, the band at 1327 cm^{-1} due to C-O stretching vibration and the band at 1444 cm^{-1} due to O-H bending vibration visible in the PGL extract were assigned to the phenolic acids also moved to the shorter frequency in the PGL-AgNPs substantiating the implication of phenolic acids as reducing and capping agents [21]. The band at 1029 cm^{-1} could be attributed to C-OH stretching vibration that arises due to presence of polysaccharides.

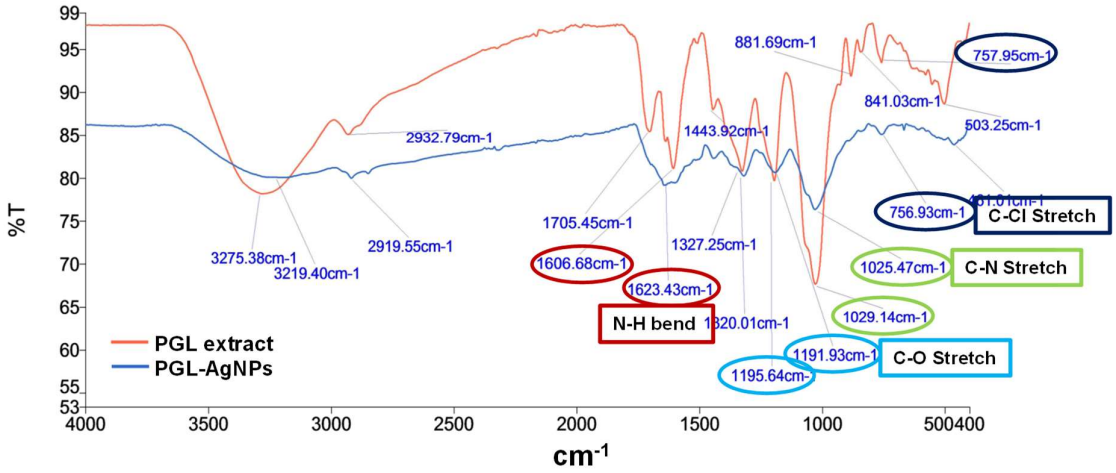

Figure 7. FTIR spectra of P. granatum leaves extract and PGL-AgNPs

2.7. Antibacterial studies

Ag^{+} and Ag salts containing silver have been used as antimicrobial agents for decades owing to their inherent microbial growth inhibition potential. The application of Ag^{+} or salts is limited due to the interfering effects of salts and requirement of uninterrupted release of sufficient concentration of Ag ion for the antimicrobial effect. These drawbacks can be surmounted by use of AgNPs as silver possess tremendous antimicrobial property as compare to other salts. Due to the greater surface area of AgNPs it would have superior binding efficiency with the microorganisms [22]. AgNPs have been suggested to exhibit antibacterial response through multiple mechanisms. One of the proposed mechanism suggests of attachment of AgNPs to the surface of the cell membrane of the bacterium, perturb its function, invaginate the bacterium followed by release of silver ions that leads to effective antibacterial activity against Gram negative bacteria [23]. Another mechanism suggests of anchorage to cell wall followed by penetration and ultimately resulting in cell death [24]. Yet another mechanism proposes release of free radicals produced by AgNPs that lead to damage to cell membrane, enhance membrane permeability, resulting in cell death [25]. However, development of economically effective strategies for production of AgNPs is highly desirable.

AgNPs have shown immense potential as antibacterial agents both against Gram negative and Gram positive bacteria [26].

In the present study, the antibacterial efficacy of PGL-AgNPs was assessed against both Gram negative and Gram positive bacteria using disc diffusion assay where ampicillin was employed as positive control [27]. An increment in the zone of inhibition was found when the concentrations of PGL-AgNPs were raised from 50 µg/ml to 200 µg/ml **(Figure 8)**. The outcomes indicate that the biosynthesized PGL-AgNPs were quite effective against both the studied Gram positive and Gram negative bacteria. Sondi *et al.* also reported inhibition of *E. coli* with a hike in AgNPs concentration and the initial number of cells used for the tests [24a]. AgNPs of 50-60 µg/cm^3 concentration exhibited 100% inhibition of growth and the cells were impaired as a result of development of cracks in the bacterial cell wall [24a]. Potent bacterial growth inhibition of *P. aeruginosa* and *E. coli* was observed at low concentrations of 25 and 50 µl using *P. granatum* leaves extract biosynthesized AgNPs [10].

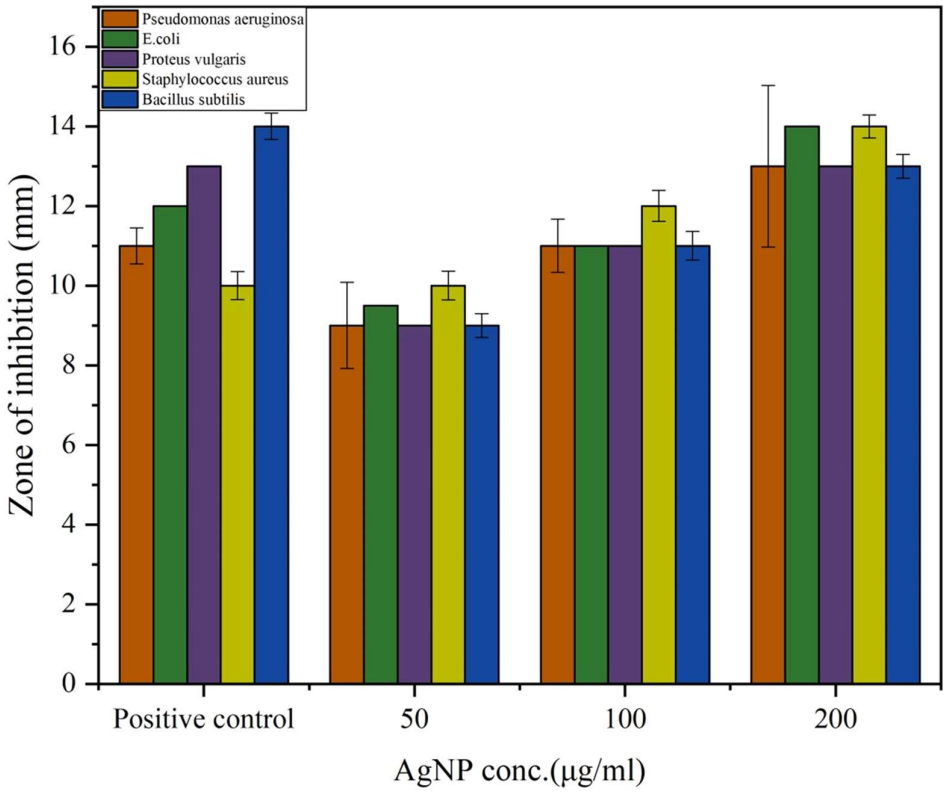

Figure 8. Antimicrobial activity of PGL-AgNPs by agar disc diffusion assay. Varying concentrations of AgNPs were investigated against five different bacteria. Graphical representation of zone of inhibition obtained using different concentration of AgNPs.

MIC was further done to detect the minimum concentration of AgNPs that can inhibit growth of bacterial culture. It was accomplished that various bacterial cultures growth can be rendered by PGL-AgNPs at concentration range of 0.050 – 0.125 mg/ml. Growth of Gram negative bacteria, namely, *E. coli, P. aeruginosa* and *P. vulgaris* were observed to be inhibited at low concentrations of AgNPs as compared to Gram positive bacteria. This could be due to presence of sturdy cell wall in the later which make accessibility of silver nanoparticles in to the cell difficult. Several research groups have reported this sort of difference in the MIC of green synthesized AgNPs [28] (Table 1). This could be due to several factors that govern the efficacy of nanoparticles including, size, surface to volume ratio, the bioactive molecules that help in reduction and synthesis of nanoparticles. None the less, in this study, PGL-AgNPs were still found to reduce the growth of Gram positive bacterial cultures, referring to much beneficial aspect of silver nanoparticles as efficient antibacterial agents.

Table 1: Determination of MIC for PGL-AgNPs against Gram positive and Gram negative bacteria

Organism	MIC (mg/ml)	Reported MIC (mg/ml)
E. coli	0.050	0.016 [28a], 0.125[28b], 0.64[28d]
P. aeruginosa	0.050	0.032[28a], 0.065[28b], 0.016[28d]
P. vulgaris	0.075	0.016[28b]
B. subtilis	0.100	0.064[28d]
S. aureus	0.125	0.128[28a], 0.125[28b], 0.625 [28c], 0.256[28d]

2.8. Mechanism of antibacterial action of PGL-AgNPs

The study of mechanism of antibacterial action of biosynthesized AgNPs was done on Gram positive bacterium- *S. aureus* as the thickness of cell wall is much greater than the Gram negative species. The biosynthesized AgNPs can easily invade the cell wall of Gram negative bacteria if the nanoparticles are capable of causing damage to Gram positive bacteria [29]. In this study, changes in bacterial membrane after the treatment of PGL-AgNPs were seen by performing FTIR spectroscopy. This technique was explored to determine the structural modifications by evaluating the changes in functional groups found in the bacterial membrane. Transmittance FTIR is quite popular for the purpose to perceive the interactions between silver nanoparticles and bacterial cell [30]. **Figure 9 A and B** illustrates the difference between membranes of PGL-AgNPs treated *S. aureus* along with proper control. The structural modifications after the treatment were predominantly classified into four regions viz. lipids (3100-2800 cm^{-1}), proteins and peptides (1800-1500 cm^{-1}), carbohydrates (1200-900 cm^{-1}) and nucleic acids (1200-600 cm^{-1}) [31]. The FTIR spectrum of treated bacteria revealed absence of peaks corresponding to nucleic acid region i.e. 1200-600 cm^{-1}. Only one peak was observed in this region which was at 1077.11 cm^{-1} falls under the category of C-O stretching of primary alcohols.

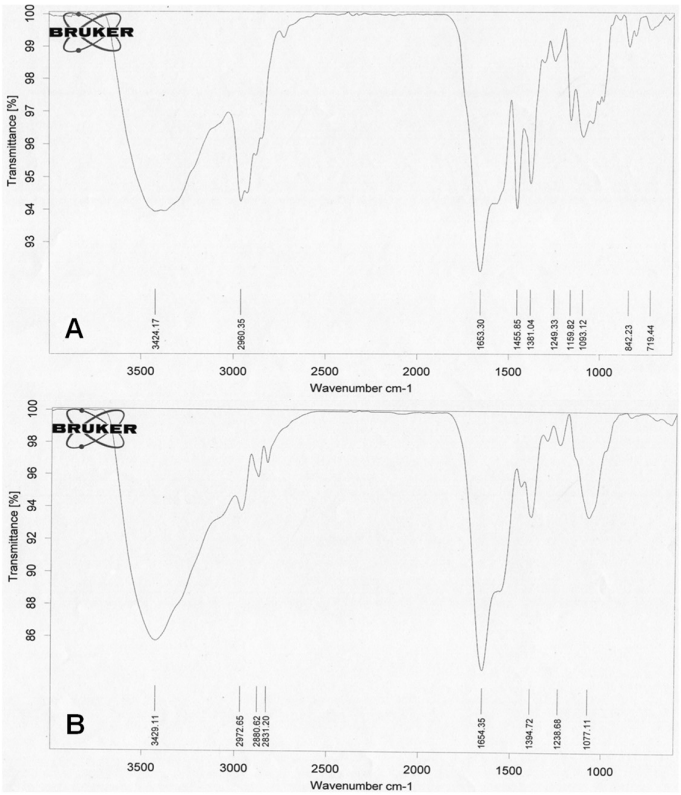

Figure 9. FTIR spectra of untreated and PGL-AgNPs treated bacterial cells

SEM scanning was also done to anticipate and compare the surface modifications in treated as well as control bacteria. In case of control (**Figure 10A)**, smooth and round surface of bacterial membrane was observed while in case of treated bacteria (**Figure 10B**); pores were observed in the cellular membrane and contents seemed to be leaked out. The reason being silver nanoparticles binds with the surface of bacterial membrane and causes various physical changes like membrane disturbances due to which content of cells leaked out.

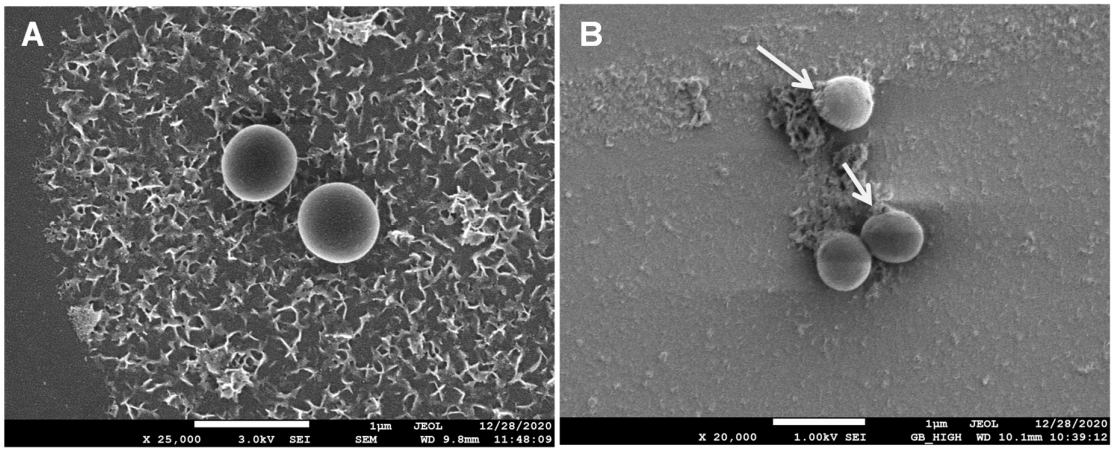

Figure 10. SEM image of untreated and PGL-AgNPs treated bacterial cells

2.9. Antibiofilm studies

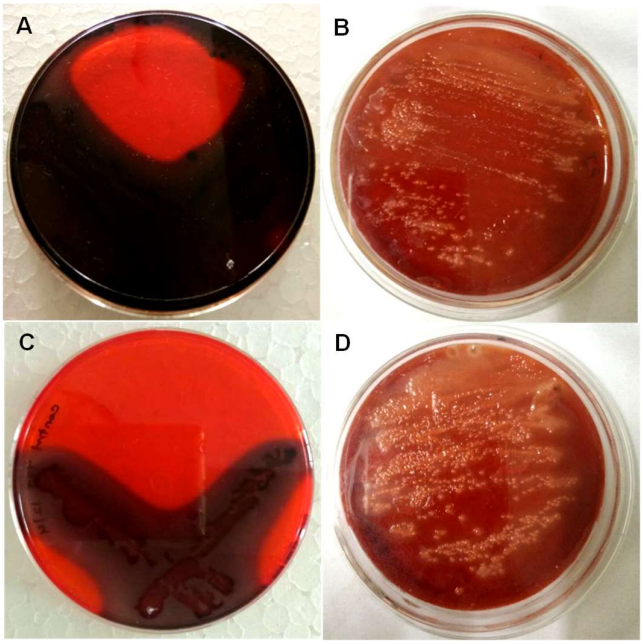

Figure 11. Assessment of the antibiofilm activity of PGL-AgNPs by CRA plate method. The appearance of black colonies (A, C) indicates the biofilm production while AgNPs treatment inhibits black colony formation. A, B- P. aeruginosa, C, D- S. aureus

The Congo red assay was performed to detect the biofilm inhibition efficacy of biosynthesized PGL-AgNPs. Biofilms facilitates the bacteria to survive in hostile conditions within or outside the host and is considered to be one of the reasons for chronic or persistent infections [32]. The Congo red dye labels the exopolysaccharides (EPS) secreted by the bacteria that are further utilized for the formation of biofilms [33]. The CRA method is fast, reproducible and the outcomes can be interpreted on the basis of color of the colony obtained. The appearance of black colored colonies exhibit

biofilm production whereas appearance of red colonies displays biofilm inhibition. Herein, two different strains i.e. *P. aeruginosa* and *S. aureus* were exposed to biosynthesized PGL-AgNPs and their biofilm formation capability was assessed. As evident from **Figure 11 (images B and D)**, the red color appeared due to inhibition of biofilm formation due to exposure of both the strains to PGL-AgNPs. In contrast, when the two strains were not treated with PGL-AgNPs they formed biofilm as evident from appearance of black color in the region of streaking **(Figure 11, A & C)**. In one of the studies Kalishwaralal *et al.* claimed inhibition of biofilm formation in *P. aeruginosa* exposed to AgNPs synthesized using *B. licheniformis* biomass, where 50 nM of AgNPs remarkably inhibited biofilm [34]. In another study, Arya *et al.* claimed inhibition of biofilm formation using biosynthesized AgNPs using *Prosopis juliflora* leaf extract in *B. subtilis* and *P. aeruginosa* [6f].

Further, to quantitate the biofilm inhibition efficacy of PGL-AgNPs, crystal violet staining was performed (**Figure 12**). As exhibited by the study, more inhibition in the formation of biofilm was seen in the bacterial strains treated with PGL-AgNPs **(Figure 12)**. As the AgNPs concentration was increased from 12.5 to 100 µg/ml greater inhibition were observed in the treated bacterial strains. Furthermore, the biofilm inhibition was noticed to be more against *P. aeruginosa* as compared to *S. aureus* at higher concentrations of AgNPs. From these studies it could be inferred that the biosynthesized PGL-AgNPs showed antibacterial effect via biofilm inhibition irrespective of the strain being Gram positive or Gram negative.

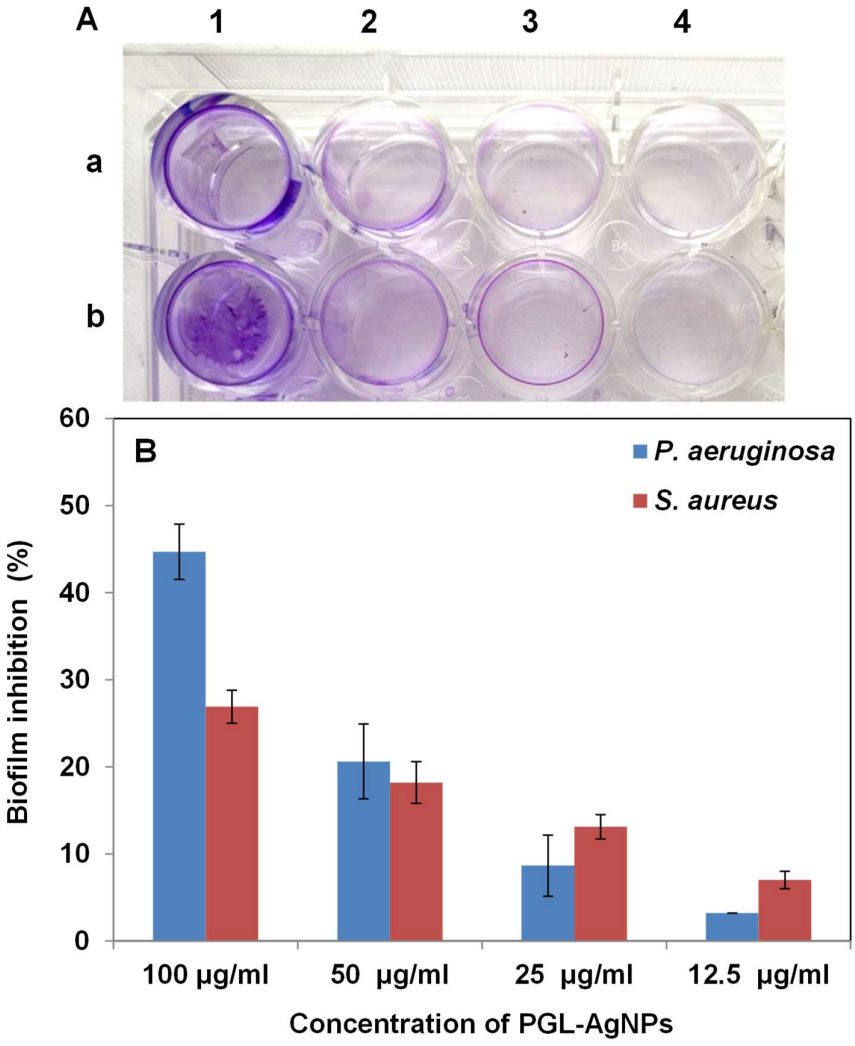

Figure 12. Assessment of the antibiofilm activity of PGL-AgNPs by crystal violet assay. The biofilm inhibition was dose dependent.

3. Methodology

2.1. Materials Required

For the biosynthesis of silver nanoparticles, silver nitrate ($AgNO_3$) was purchased from Merck Limited, India. Lyophilized culture of *Escherichia coli* (MTCC 40), *Pseudomonas aeruginosa* (MTCC 424), *Proteus vulgaris* (MTCC 426), *Bacillus subtilis* (MTCC 441), *Staphylococcus aureus* (MTCC 739), were acquired from the Microbial Type Culture Collection Center (MTCC) placed at Institute of Microbial Technology (IMTECH) Chandigarh, India. Nutrient broth and Nutrient agar procured from Hi-Media Laboratories, India.

3.2. Preparation of leaves extract

Punica granatum leaves were freshly collected from the neighborhood of campus of The IIS University, Jaipur, Rajasthan, India 26.9124°N, 75.7873° E and identified. Fresh leaves of *P. granatum* were collected and washed twice with double distilled water to remove dirt from the surface. Clean leaves were shade dried for 15 days followed by crushing with mortar and pestle. 5% aqueous extract solution was prepared by boiling 5g leaves powder in 100 ml of deionized water for 15-20 min. The solution was left at room temperature to cool. Whatman filter paper No. 1 was then used to filter the prepared extract and stored at 4°C till further requirement.

3.3. Biosynthesis of silver nanoparticles

The biosynthesis of PGL-AgNPs was achieved by drop-wise addition of the leaf extract into aqueous $AgNO_3$ solution with uninterrupted stirring at 600 rpm. The reaction was allowed to proceed till a color change was observed. After the stabilization of color, synthesized AgNPs were isolated by centrifugation at 10,000 rpm (ST16R, Sorvall, Thermo Scientific) for 10 min. The isolated nanoparticles were washed by re-dispersing them in deionized water.

3.4. UV-visible spectroscopic analysis

After observing color change, the freshly biosynthesized sample was subjected to UV-visible spectrophotometric analysis. The reduction of silver ions (Ag^+) by biomolecules in aqueous solution was observed by taking absorbance in the range 300-700 nm using spectrophotometer (Multiskan go, Thermo Scientific, USA).

3.5. Box-Behnken design for optimization of parameters for biosynthesis of PGL-AgNPs

The efficient optimization of PGL-AgNPs was achieved using Box-Behnken design provided by Design Expert ver. 12.0 software (Stat-Ease Inc., Minneapolis, USA). Different parameters that control the synthesis of AgNPs were optimized, that includes concentration of $AgNO_3$(mM), reaction temperature (°C) and ratio of concentration of extract to $AgNO_3$ (µl). These parameters were taken as independent factors for two-level i.e., low (-1) and high (+1), optimization process (**Table 1**). Based upon the preferred design, the model suggested 17 experimental trial runs for optimization of PGL-AgNPs given in **table 2**. The analysis of particles size and polydispersity index (PDI) generated as responses (dependent factors) was the main reason behind this systematic optimization using BBD.

Table 1: Independent variables taken for systematic optimization by Box-Behnken design

S. No.	Independent variables	Units	Low value	High value
1	$AgNO_3$ concentration	Millimolar (mM)	0.5	2.5
2	Extract to $AgNO_3$ ratio	Microlitre (µl)	50	200
3	Temperature	Celsius (°C)	20	50

Table 2: Experimental trial runs given by Box- Behnken Design

Trial run	$AgNO_3$ concentration (mM)	Extract to $AgNO_3$ ratio(µl)	Reaction temperature (°C)	Particles size(nm)	PDI
1	2.5	125	20	101.061	0.921023
2	2.5	50	35	94.7784	0.153355
3	1.5	50	50	104.04	0.0763458
4	0.5	125	50	96.7092	0.38042
5	0.5	125	20	105.727	0.894881
6	1.5	125	35	106.139	0.341596
7	2.5	125	50	105.371	0.794349
8	1.5	125	35	102.797	0.626777
9	2.5	200	35	107.711	0.832383
10	0.5	200	35	103.869	0.607419
11	1.5	200	20	101.378	0.64091
12	1.5	200	50	101.686	0.0149703
13	1.5	125	35	98.7829	0.32121
14	1.5	125	35	91.7955	0.633585
15	1.5	125	35	92.7959	0.53263
16	1.5	50	20	109.783	0.383734
17	0.5	50	35	95.368	0.36545

3.6. Physicochemical characterization of PGL-AgNPs

Morphological and size characterization of biosynthesized PGL-AgNPs was done by SEM (JEOL, 7400F, Tokyo, Japan). The existence of silver element was proved by EDX analysis. Zetasizer Nano ZS with laser Doppler velocimetry was used to measure zeta potential of sample that was done automatically-in triplicates. Also, the crystalline nature of biosynthesized AgNPs was resolved by XRD. For the analysis of functional group, desiccated samples of extract and PGL-AgNPs were assessed by FTIR spectrometer (Perkin Elmer, Yokohama, Japan).The disc of PGL-AgNPs was prepared with KBr. The scanning was done in the range of 4000 to 400 cm^{-1}at 2 cm^{-1} resolution keeping KBr pellet as blank. The presence of functional groups and their interactions were detected by FTIR spectrum.

3.7. Antibacterial studies

Antibacterial activity has been tested on Gram positive and Gram-negative bacteria, viz. *E.coli*, *S. aureus*, *P. aeruginosa*, *P. vulgaris*, *B. subtilis* by disc diffusion method [27]. The lyophilized cultures were revived using nutrient broth and kept at 37°C overnight to attain optimum $O.D._{600}$ (0.4) for further use. Each plate was inoculated with 20 µl of culture and swabbed over entire agar surface using sterilized cotton swabs. PGL-AgNPs (50µg, 100µg, 200µg), *P. gratanum* extract (10%) as negative control and ampicillin (100µg/µl) as positive control were used. Autoclaved filter paper discs loaded with varying concentrations of PGL-AgNPs were placed on the inoculated agar medium. Petri plates were then incubated overnight at 37°C for the growth of the cultures. Zone of inhibition was deliberated in mm using standardized scale around the disc impregnated with PGL-AgNPs, plant extract and ampicillin.

In order to determine minimal inhibitory concentration (MIC) of biosynthesized PGL-AgNPs, standard broth dilution method was method of choice[35]. In the corresponding methodology, the antibacterial efficacy of PGL-AgNPs was studied against *E. coli, P. aeruginosa, P. vulgaris, B. subtilis* and *S. aureus* by observing the bacterial growth liquid broth medium. Silver nanoparticles were used in varying concentrations with range 0.010 mg/ml to 0.250 mg/ml. The microorganisms culture taken for analysis were of absorbance 0.5 at 600 nm (0.5 McFarland's standard) and no

nanoparticles, only broth was added to control cultures. The cultures were incubated at 37°C for 24h. The lowest concentration of PGL-AgNPs at which no growth was visible or observed at 600 nm was considered as MIC for PGL-AgNPs against those bacteria.

3.8. Mechanism of antibacterial action of PGL-AgNPs

With an aim to understand the antibacterial mechanism of biosynthesized PGL-AgNPs on bacterium, FTIR and SEM were performed to observe the morphological changes in *S. aureus*. For FTIR, overnight grown PGL-AgNPs treated cultures along with proper control were taken. After the incubation, bacterial cells were collected in pellets after centrifugation and left on desiccator to dry. The dried samples were then used to generate FTIR spectra. Similarly, overnight grown cultures as mentioned above were used to prepare glass slides for SEM analysis. Heat fixed smear of bacterial cultures were allowed to stain with 2.5% glutaraldehyde for 30 min followed by washing with phosphate buffer. The dehydration of the fixed samples was attained by drowning them in ascending percentage of ethanol solution for 15 min each. Lastly, samples were left at 37°C for 1hto dehydrate completely. Thin coating of gold (<5 nm) was done before the SEM analysis [36].

3.9. Antibiofilm studies

Investigation of the biofilm inhibition property of AgNPs was done using Congo red agar method (CRA) as reported by Freeman and group [33] . *P. aeruginosa* and *S. aureus* strains were cultivated on Luria Bertani (LB) broth provided with an incubation temperature of 37°C for 24h. Brain heart infusion (BHI) agar media was prepared, enriched with 5% sucrose (w/v) and 0.08% Congo red dye (w/v). All the media constituents were added and autoclaved while Congo red was separately autoclaved and then added to media at a temperature of 55°C. Suspensions of PGL-AgNPs of increasing concentrations of 5, 10, 20, 40, 80, 100µg/mL were made with distilled water and were spread onto separate solidified agar plates and allowed to diffuse for 6-10 min. The 2-way streaking of strains were done separately and incubated at 37°C under aerobic conditions for 24h. The biofilm producer strains are supposed to form black colonies, while the biofilm inhibition results in red colonies.

To quantitate the biofilm inhibition efficacy of biosynthesized PGL-AgNPs, they were exposed to *P. aeruginosa* and *S. aureus* followed by incorporation of crystal violet dye. 12-14h grown cultures diluted 1:100 (v/v) in fresh medium were transferred to wells (200 µl) of 96-well tissue culture plate (TCP), and incubated for 16h at 37°C without shaking. Suspension of PGL-AgNPs (10µl) was added to each well at 4 different concentrations (100 µg/ml, 50 µg/ml, 25 µg/ml, 12.5 µg/ml). After measuring OD_{600}, the planktonic cells were poured out, and plates were washed with 200µl of PBS (pH 7.2) to eradicate non-adherent bacteria and left to dried up for 10 minutes. Post drying, 200 µl of crystal violet (0.1%, w/v) was supplemented to each well and left for 10 min to stain adherent biofilms. After staining wells were then washed with deionized water to clear surplus stain and the dye integrated with adherent cells was dissolved by 95% ethanol. Lastly, the absorbance was taken at 595 nm on Elisa plate reader.

The percentage inhibition of biofilm formation was obtained by calculating the absorbance discrepancy between treated and control wells. The base controls kept were 200µl of crystal violet, 200µl of ethanol the percent reduction in growth was measured to evaluate the level of inhibition in growth of biofilm.

3.10. Statistical analysis

All the experimental analyses were carried out in triplicates, with three separate experiments to describe reproducibility. All procured experimental data were provided as mean ± standard deviation (±SD).

4. Conclusion

In the prevailing investigation, we efficiently biosynthesized AgNPs using leaves extract of

Punica granatum. The study revealed that optimal size distribution nanoparticles can be synthesized at 31.4°C when the concentration of $AgNO_3$ is 1.5 mM, with extract volume of 55.55 µl was taken and reaction continued for 15 min. Physicochemical characterization studies via SEM, DLS revealed that the PGL-AgNPs were spherical and of ~ 37.5 nm in size with uniform distribution and zeta potential of -34 mV. The AgNPs exhibited effective antibacterial efficacy against the studied Gram positive and Gram negative bacteria as revealed by disc diffusion method. The zone of inhibition observed for bacteria, *S. aureus*, *B. subtilis*, *P. aeruginosa*, *E. coli*, and *P. vulgaris* was 14, 13, 14, 13 and 13 mm, respectively when 200 µg/ml of nanoparticles were employed. Further, antibiofilm efficacy of PGL-AgNPs was estimated using Congo red assay and Crystal violet staining. The biofilm inhibition was higher as the concentrations of AgNPs were escalated from 12.5 to 100 µg/ml. The FT-IR and SEM studies depicted the bacterial and PGL-AgNPs interaction showing membrane disruptions in Gram positive bacteria. These studies propose PGL-AgNPs as potent antibacterial and antibiofilm candidate that can be explored for *in vivo* as well as therapeutic applications.

Author contributions: Conceptualization, Ajeet Kumar, Asad Syed, Nidhi Gupta and Surendra Nimesh; Data curation, Monisha Singhal; Formal analysis, Sreemoyee Chatterjee, Asad Syed, Ali H Bahkali, Nidhi Gupta and Surendra Nimesh; Funding acquisition, Surendra Nimesh; Methodology, Monisha Singhal and Sreemoyee Chatterjee; Project administration, Nidhi Gupta and Surendra Nimesh; Resources, Ajeet Kumar, Ali H Bahkali and Surendra Nimesh; Supervision, Nidhi Gupta and Surendra Nimesh; Visualization, Asad Syed, Nidhi Gupta and Surendra Nimesh; Writing – original draft, Monisha Singhal; Writing – review & editing, Asad Syed, Ali H Bahkali, Nidhi Gupta and Surendra Nimesh.

Funding: Surendra Nimesh acknowledges the financial assistance from Department of Biotechnology (DBT) (grant no. 6242-P82/ RGCB/PMD/DBT/SNMH/2015), Government of India. Ali H. Bahkali acknowledges the financial assistance form Researchers Supporting Project number (RSP-2021/15), King Saud University, Riyadh, Saudi Arabia.

Conflicts of Interest: The authors declare no conflict of interest.

References

1. (a) Yumak, T.; Kuralay, F.; Muti, M.; Sinag, A.; Erdem, A.; Abaci, S., Preparation and characterization of zinc oxide nanoparticles and their sensor applications for electrochemical monitoring of nucleic acid hybridization. *Colloids and Surfaces B: Biointerfaces* **2011,** *86* (2), 397-403; (b) Medhat, D.; Hussein, J.; El-Naggar, M. E.; Attia, M. F.; Anwar, M.; Latif, Y. A.; Booles, H. F.; Morsy, S.; Farrag, A. R.; Khalil, W. K., Effect of Au-dextran NPs as anti-tumor agent against EAC and solid tumor in mice by biochemical evaluations and histopathological investigations. *Biomedicine & Pharmacotherapy* **2017,** *91*, 1006-1016.
2. Hebeish, A.; El-Naggar, M.; Fouda, M. M.; Ramadan, M.; Al-Deyab, S. S.; El-Rafie, M., Highly effective antibacterial textiles containing green synthesized silver nanoparticles. *Carbohydrate Polymers* **2011,** *86* (2), 936-940.
3. Ahmad, N.; Sharma, S.; Alam, M. K.; Singh, V.; Shamsi, S.; Mehta, B.; Fatma, A., Rapid synthesis of silver nanoparticles using dried medicinal plant of basil. *Colloids and Surfaces B: Biointerfaces* **2010,** *81* (1), 81-86.
4. (a) Mohanpuria, P.; Rana, N. K.; Yadav, S. K., Biosynthesis of nanoparticles: technological concepts and future applications. *Journal of nanoparticle research* **2008,** *10* (3), 507-517; (b) Saratale, R. G.; Karuppusamy, I.; Saratale, G. D.; Pugazhendhi, A.; Kumar, G.; Park, Y.; Ghodake, G. S.; Bharagava, R. N.; Banu, J. R.; Shin, H. S., A comprehensive review on green nanomaterials using biological systems: Recent perception and their future applications. *Colloids Surf B Biointerfaces* **2018,** *170*, 20-35; (c) Saratale, R. G.; Saratale, G. D.; Shin, H. S.; Jacob, J. M.; Pugazhendhi, A.; Bhaisare, M.; Kumar, G., New insights on the green synthesis of metallic nanoparticles using plant and waste biomaterials: current knowledge, their agricultural and environmental applications. *Environ Sci Pollut Res Int* **2018,** *25* (11), 10164-10183.
5. Valli, J. S.; Vaseeharan, B., Biosynthesis of silver nanoparticles by Cissus quadrangularis extracts. *Materials Letters* **2012,** *82*, 171-173.
6. (a) Arya, G.; Kumari, R. M.; Gupta, N.; Kumar, A.; Chandra, R.; Nimesh, S., Green synthesis of silver nanoparticles using Prosopis juliflora bark extract: reaction optimization, antimicrobial and catalytic activities. *Artificial cells, nanomedicine, and biotechnology* **2017**, 1-9; (b) Arya, G.; Sharma, N.; Ahmed, J.;

Gupta, N.; Kumar, A.; Chandra, R.; Nimesh, S., Degradation of anthropogenic pollutant and organic dyes by biosynthesized silver nano-catalyst from Cicer arietinum leaves. *Journal of Photochemistry and Photobiology B: Biology* **2017,** *174*, 90-96; (c) Goyal, S.; Gupta, N.; Kumar, A.; Chatterjee, S.; Nimesh, S. Antibacterial, anticancer and antioxidant potential of silver nanoparticles engineered using Trigonella foenum-graecum seed extract *IET Nanobiotechnology* [Online], 2018. http://digital-library.theiet.org/content/journals/10.1049/iet-nbt.2017.0089; (d) Mohan Kumar, K.; Sinha, M.; Mandal, B. K.; Ghosh, A. R.; Siva Kumar, K.; Sreedhara Reddy, P., Green synthesis of silver nanoparticles using Terminalia chebula extract at room temperature and their antimicrobial studies. *Spectrochim Acta A Mol Biomol Spectrosc* **2012,** *91*, 228-33; (e) Edison, T. J.; Sethuraman, M. G., Biogenic robust synthesis of silver nanoparticles using Punica granatum peel and its application as a green catalyst for the reduction of an anthropogenic pollutant 4-nitrophenol. *Spectrochim Acta A Mol Biomol Spectrosc* **2013,** *104*, 262-4; (f) Arya, G.; Kumari, R. M.; Sharma, N.; Gupta, N.; Kumar, A.; Chatterjee, S.; Nimesh, S., Catalytic, antibacterial and antibiofilm efficacy of biosynthesised silver nanoparticles using Prosopis juliflora leaf extract along with their wound healing potential. *Journal of Photochemistry and Photobiology B: Biology* **2019,** *190*, 50-58; (g) Arya, G.; Kumari, R. M.; Sharma, N.; Chatterjee, S.; Gupta, N.; Kumar, A.; Nimesh, S., Evaluation of antibiofilm and catalytic activity of biogenic silver nanoparticles synthesized from Acacia nilotica leaf extract. *Advances in Natural Sciences: Nanoscience and Nanotechnology* **2018,** *9* (4), 045003.

7. (a) Saratale, G. D.; Saratale, R. G.; Kim, D. S.; Kim, D. Y.; Shin, H. S., Exploiting Fruit Waste Grape Pomace for Silver Nanoparticles Synthesis, Assessing Their Antioxidant, Antidiabetic Potential and Antibacterial Activity Against Human Pathogens: A Novel Approach. *Nanomaterials (Basel)* **2020,** *10* (8); (b) Saratale, R. G.; Saratale, G. D.; Ghodake, G.; Cho, S. K.; Kadam, A.; Kumar, G.; Jeon, B. H.; Pant, D.; Bhatnagar, A.; Shin, H. S., Wheat straw extracted lignin in silver nanoparticles synthesis: Expanding its prophecy towards antineoplastic potency and hydrogen peroxide sensing ability. *Int J Biol Macromol* **2019,** *128*, 391-400.
8. Husen, A.; Siddiqi, K. S., Plants and microbes assisted selenium nanoparticles: characterization and application. *Journal of nanobiotechnology* **2014,** *12* (1), 28.
9. Saratale, R. G.; Shin, H. S.; Kumar, G.; Benelli, G.; Kim, D.-S.; Saratale, G. D., Exploiting antidiabetic activity of silver nanoparticles synthesized using Punica granatum leaves and anticancer potential against human liver cancer cells (HepG2). *Artificial Cells, Nanomedicine, and Biotechnology* **2018,** *46* (1), 211-222.
10. Devanesan, S.; AlSalhi, M. S.; Balaji, R. V.; Ranjitsingh, A. J. A.; Ahamed, A.; Alfuraydi, A. A.; AlQahtani, F. Y.; Aleanizy, F. S.; Othman, A. H., Antimicrobial and Cytotoxicity Effects of Synthesized Silver Nanoparticles from Punica granatum Peel Extract. *Nanoscale Res Lett* **2018,** *13* (1), 315.
11. Mehra, A.; Chauhan, S.; Jain, V. K.; Nagpal, S., Nanoparticles of Punicalagin Synthesized from Pomegranate (Punica Granatum L.) with Enhanced Efficacy Against Human Hepatic Carcinoma Cells. *Journal of Cluster Science* **2021**.
12. Ahmed, Q.; Gupta, N.; Kumar, A.; Nimesh, S., Antibacterial efficacy of silver nanoparticles synthesized employing Terminalia arjuna bark extract. *Artificial cells, nanomedicine, and biotechnology* **2017,** *45* (6), 1-9.
13. Veisi, H.; Azizi, S.; Mohammadi, P., Green synthesis of the silver nanoparticles mediated by Thymbra spicata extract and its application as a heterogeneous and recyclable nanocatalyst for catalytic reduction of a variety of dyes in water. *Journal of Cleaner Production* **2018,** *170*, 1536-1543.
14. Sunkar, S.; Nachiyar, C. V., Biogenesis of antibacterial silver nanoparticles using the endophytic bacterium Bacillus cereus isolated from Garcinia xanthochymus. *Asian Pac J Trop Biomed* **2012,** *2* (12), 953-9.
15. Chand, K.; Cao, D.; Eldin Fouad, D.; Hussain Shah, A.; Qadeer Dayo, A.; Zhu, K.; Nazim Lakhan, M.; Mehdi, G.; Dong, S., Green synthesis, characterization and photocatalytic application of silver nanoparticles synthesized by various plant extracts. *Arabian Journal of Chemistry* **2020,** *13* (11), 8248-8261.
16. Krupa, A. N. D.; Abigail, M. E. A.; Santhosh, C.; Grace, A. N.; Vimala, R., Optimization of process parameters for the microbial synthesis of silver nanoparticles using 3-level Box–Behnken Design. *Ecological Engineering* **2016,** *87*, 168-174.
17. (a) He, S.; Yao, J.; Jiang, P.; Shi, D.; Zhang, H.; Xie, S.; Pang, S.; Gao, H., Formation of silver nanoparticles and self-assembled two-dimensional ordered superlattice. *Langmuir* **2001,** *17* (5), 1571-1575; (b) Bohren, C. F.; Huffman, D. R., *Absorption and scattering by a sphere*. Wiley Online Library: 1983.

18. Mie, G., Contributions to the optics of turbid media, particularly of colloidal metal solutions. *Contributions to the optics of turbid media, particularly of colloidal metal solutions Transl. into ENGLISH from Ann. Phys.(Leipzig), v. 25, no. 3, 1908 p 377-445* **1976**.
19. Yazdi, T.; Ehsan, M.; Khara, J.; Sadeghnia, H. R.; Esmaeilzadeh Bahabadi, S.; Darroudi, M., Biosynthesis, characterization, and antibacterial activity of silver nanoparticles using Rheum turkestanicum shoots extract. *Research on Chemical Intermediates* **2018,** *44* (2), 1325-1334.
20. Patra, S.; Mukherjee, S.; Barui, A. K.; Ganguly, A.; Sreedhar, B.; Patra, C. R., Green synthesis, characterization of gold and silver nanoparticles and their potential application for cancer therapeutics. *Mater Sci Eng C Mater Biol Appl* **2015,** *53*, 298-309.
21. Das, B.; De, A.; Das, M.; Das, S.; Samanta, A., A new exploration of Dregea volubilis flowers: Focusing on antioxidant and antidiabetic properties. *South African Journal of Botany* **2017,** *109*, 16-24.
22. Rai, M.; Yadav, A.; Gade, A., Silver nanoparticles as a new generation of antimicrobials. *Biotechnol Adv* **2009,** *27* (1), 76-83.
23. Morones, J. R.; Elechiguerra, J. L.; Camacho, A.; Holt, K.; Kouri, J. B.; Ramirez, J. T.; Yacaman, M. J., The bactericidal effect of silver nanoparticles. *Nanotechnology* **2005,** *16* (10), 2346-53.
24. (a) Sondi, I.; Salopek-Sondi, B., Silver nanoparticles as antimicrobial agent: a case study on E. coli as a model for Gram-negative bacteria. *J Colloid Interface Sci* **2004,** *275* (1), 177-82; (b) Shrivastava, S.; Bera, T.; Roy, A.; Singh, G.; Ramachandrarao, P.; Dash, D., Characterization of enhanced antibacterial effects of novel silver nanoparticles. *Nanotechnology* **2007,** *18* (22), 225103.
25. Kim, J. S.; Kuk, E.; Yu, K. N.; Kim, J. H.; Park, S. J.; Lee, H. J.; Kim, S. H.; Park, Y. K.; Park, Y. H.; Hwang, C. Y.; Kim, Y. K.; Lee, Y. S.; Jeong, D. H.; Cho, M. H., Antimicrobial effects of silver nanoparticles. *Nanomedicine* **2007,** *3* (1), 95-101.
26. (a) MubarakAli, D.; Thajuddin, N.; Jeganathan, K.; Gunasekaran, M., Plant extract mediated synthesis of silver and gold nanoparticles and its antibacterial activity against clinically isolated pathogens. *Colloids Surf B Biointerfaces* **2011,** *85* (2), 360-5; (b) Das, B.; Dash, S. K.; Mandal, D.; Ghosh, T.; Chattopadhyay, S.; Tripathy, S.; Das, S.; Dey, S. K.; Das, D.; Roy, S., Green synthesized silver nanoparticles destroy multidrug resistant bacteria via reactive oxygen species mediated membrane damage. *Arabian Journal of Chemistry*; (c) Kaviya, S.; Santhanalakshmi, J.; Viswanathan, B.; Muthumary, J.; Srinivasan, K., Biosynthesis of silver nanoparticles using citrus sinensis peel extract and its antibacterial activity. *Spectrochim Acta A Mol Biomol Spectrosc* **2011,** *79* (3), 594-8.
27. Magaldi, S.; Mata-Essayag, S.; De Capriles, C. H.; Perez, C.; Colella, M.; Olaizola, C.; Ontiveros, Y., Well diffusion for antifungal susceptibility testing. *International Journal of Infectious Diseases* **2004,** *8* (1), 39-45.
28. (a) Javan Bakht Dalir, S.; Djahaniani, H.; Nabati, F.; Hekmati, M., Characterization and the evaluation of antimicrobial activities of silver nanoparticles biosynthesized from Carya illinoinensis leaf extract. *Heliyon* **2020,** *6* (3), e03624; (b) Raheem, H. Q.; Al-Thahab, A.; Abd, F. G., Antibacterial activity of silver nanoparticles extracted from Proteus mirabilis and healing the wound in rabbit. *Biochem. Cell. Arch.* **2018,** *18* (1), 97-104; (c) Parvekar, P.; Palaskar, J.; Metgud, S.; Maria, R.; Dutta, S., The minimum inhibitory concentration (MIC) and minimum bactericidal concentration (MBC) of silver nanoparticles against Staphylococcus aureus. *Biomater Investig Dent* **2020,** *7* (1), 105-109; (d) Wypij, M.; Czarnecka, J.; Swiecimska, M.; Dahm, H.; Rai, M.; Golinska, P., Synthesis, characterization and evaluation of antimicrobial and cytotoxic activities of biogenic silver nanoparticles synthesized from Streptomyces xinghaiensis OF1 strain. *World J Microbiol Biotechnol* **2018,** *34* (2), 23.
29. Kora, A. J.; Sashidhar, R. B., Biogenic silver nanoparticles synthesized with rhamnogalacturonan gum: Antibacterial activity, cytotoxicity and its mode of action. *Arabian Journal of Chemistry* **2018,** *11* (3), 313-323.
30. Tyagi, P.; Singh, M.; Kumari, H.; Kumari, A.; Mukhopadhyay, K., Bactericidal activity of curcumin I is associated with damaging of bacterial membrane. *PLoS One* **2015,** *10* (3), e0121313.
31. (a) Jiang, W.; Yang, K.; Vachet, R. W.; Xing, B., Interaction between Oxide Nanoparticles and Biomolecules of the Bacterial Cell Envelope As Examined by Infrared Spectroscopy. *Langmuir* **2010,** *26* (23), 18071-18077; (b) Eckhardt, S.; Brunetto, P. S.; Gagnon, J.; Priebe, M.; Giese, B.; Fromm, K. M., Nanobio silver: its interactions with peptides and bacteria, and its uses in medicine. *Chem Rev* **2013,** *113* (7), 4708-54; (c) Fang, J.; Lyon, D. Y.; Wiesner, M. R.; Dong, J.; Alvarez, P. J., Effect of a fullerene water suspension on bacterial phospholipids and membrane phase behavior. *Environ Sci Technol* **2007,** *41* (7), 2636-42.

32. Christensen, G. D.; Simpson, W. A.; Younger, J. J.; Baddour, L. M.; Barrett, F. F.; Melton, D. M.; Beachey, E. H., Adherence of coagulase-negative staphylococci to plastic tissue culture plates: a quantitative model for the adherence of staphylococci to medical devices. *J Clin Microbiol* **1985,** *22* (6), 996-1006.
33. Freeman, D. J.; Falkiner, F. R.; Keane, C. T., New method for detecting slime production by coagulase negative staphylococci. *J Clin Pathol* **1989,** *42* (8), 872-4.
34. Kalishwaralal, K.; BarathManiKanth, S.; Pandian, S. R.; Deepak, V.; Gurunathan, S., Silver nanoparticles impede the biofilm formation by Pseudomonas aeruginosa and Staphylococcus epidermidis. *Colloids Surf B Biointerfaces* **2010,** *79* (2), 340-4.
35. Sosa, I. O.; Noguez, C.; Barrera, R. G., Optical Properties of Metal Nanoparticles with Arbitrary Shapes. *The Journal of Physical Chemistry B* **2003,** *107* (26), 6269-6275.
36. Chatterjee, S.; Shekhawat, K.; Gupta, N., Bioreduction of toxic hexavalent chromium by novel indigenous microbe Brevibacillus agri isolated from tannery wastewater. *International Journal of Environmental Science and Technology* **2019,** *16* (7), 3549-3556.